Scanning Microscopy Vol. 12, No. 1, 1998 (Pages 3-8) 0891-7035/98$5.00+.25
Scanning Microscopy International, Chicago (AMF O'Hare), IL 60666 USA

NUCLEATION, GROWTH AND COARSENING IN PHASE-SEPARATING SYSTEMS

Celeste Sagui, Dean Stinson O'Gorman and Martin Grant*

Centre for the Physics of Materials, Physics Department, Rutherford Building,
McGill University, 3600 rue University, Montréal, Quebec, Canada H3A 2T8

(Received for publication May 13, 1996 and in revised form September 25, 1996)

Abstract

In this work, we have re-examined the classical problem of nucleation and growth. A new model considers the correlations between droplets and naturally incorporates the crossover from the early-stage, nucleation-dominated regime to the scaling, late-stage, coarsening regime within a single framework. Results are reported for three-dimensional growth in three dimensions, and the growth of two-dimensional droplets on a two-dimensional substrate. Since the method involves only interface equations, it permits the simulation of much larger systems than can be studied using other methods. In particular, results are given for the variation with time of the number of droplets, the excess supersaturation, and the droplet distribution function, for different concentrations and temperatures.

Key Words: Metastability, phase separation, nucleation, growth, Ostwald ripening, scaling.

*Contact for correspondence:
Martin Grant, address as above.
Telephone number: (514) 398-6525
FAX number: (514) 398-6526
E-mail: grant@physics.mcgill.ca

Introduction

Metastable states decay towards equilibrium via the introduction of finite-size fluctuations. The energy for the formation of a droplet of the stable phase is determined by the competition between the volume energy (which favors growth) and the droplet surface energy (which favors dissolution). This competition defines a critical size R_c for nucleation of a droplet. The kinetics of phase separation from such a metastable state has been intensively studied and the early stages of nucleation [2, 3, 4, 6, 7, 8, 9, 17] and late stages of coarsening [11] are well understood. Much less, however, is known about the cross-over regime. In 1980, Langer and Schwartz [10] used a mean-field approach to study the non-linear dynamical equations of motion for a phase separating system for the entire time regime. The importance of a theoretical description that includes the correlation effects has been emphasized by the abundant experimental data on these processes [14, 15, 19]. Moreover, the growing interest in the formation of clusters on surfaces calls for new theoretical developments to account for the increasing number of experimental results reported [21].

Here, we report on a study of the decay of metastable states, which involves a model of self-consistent equations to describe nucleation, growth and coarsening in phase separating systems. Our approach has combined steady-state homogeneous nucleation theory with classical Lifshitz-Slyozov theory (Ostwald ripening) [11], modified to account for the correlations among the droplets. This new formalism naturally incorporates the cross-over from the early-stage nucleation to the late-stage scaling regime without *ad-hoc* assumptions. We have performed simulations of the entire time regime for two-dimensional domains (in dimension d = 2) and three-dimensional domains (in d = 3).

Model

In this section, we restrict the equations to d = 3. We introduce the capillary length $l_c = 2\sigma\nu_m/(kT)$ and the characteristic time $\tau_c = l/\{DC_{eq}(\infty)\nu_m\}$; τ_c is the time it takes a monomer to diffuse over a distance comparable to the capillary length. These quantities involve the surface tension σ, the molecular volume ν_m, the temperature T, the Boltzmann

constant k, the solute concentration in the matrix at a planar interface $C_{eq}(\infty)$, and the diffusion constant D. We also introduce a dimensionless concentration field $\theta(r,t) = \{C(\mathbf{r},t)-C_{eq}(\infty)\}/C_{eq}(\infty)$. Its value, far from any droplet, is the time-dependent supersaturation $\chi(t)$. The energy of a droplet of radius R' is thus given by: $E(R')/kT = 4\pi\sigma\{R'^2 - 2\chi(t)R'^3/(3l_c)\}$. Minimization of this energy with respect to R' gives the critical radius for nucleation of a droplet, R'. In our study, we will express units of length and time in terms of l_c and τ_c. Thus, the (dimensionless) critical radius is given by $R_c = R'/l_c = 1/\chi(t)$. The height of the nucleation barrier is given by E(R') evaluated at the critical radius: $E_c/kT = \{\chi_0/\chi(t)\}^2$, where $\chi = (4\pi\sigma l)/(3kT)$ [10]. In terms of these quantities, the field-theoretic steady-state nucleation rate in d = 3 can be written in dimensionless form as [5]:

$$J_3 = A_3\left(\frac{\chi(t)}{\chi_0}\right)^{2/3}\left(1+\frac{\chi(t)}{\chi_0}\right)^{3.55}\exp\left[-\left(\frac{\chi_0}{\chi(t)}\right)^2\right] \qquad (1)$$

The nucleation rate represents the number of droplets nucleated per unit volume per unit time for a given supersaturation. In the simulations, the radius of every newly nucleated droplet is chosen from a gaussian distribution centered at R_c, with a width dR_c.

The time evolution of the system is given by the solution of the multi-droplet diffusion equation for the concentration field $\theta(r,t)$. In the monopole approximation [18, 20]:

$$\frac{\partial\theta(r,t)}{\partial t} - \nabla^2\theta(r,t) = -4\pi\sum_{i=1}^{N(t)} Q_i\delta(r-r_i) \qquad (2)$$

where the coefficients Q_i describe the strength of the source or sink of the current for diffusion. We assume spherical droplets in local equilibrium: the concentration near the interface is determined by the local curvature and the local surface tension. This is the Gibbs-Thomson boundary condition $\theta(\mathbf{R}_i) = l/R_i$ [21]. An approximate solution for Eq. (2) in terms of the N coefficients Q_i and an integration coefficient Q_0, that takes into account the time evolution of the supersaturation $\chi(t)$, is evaluated on the surface of droplet i:

$$\frac{1}{R_i} - \frac{1}{\overline{R}(t)} = Q_0(t) - \sum_{j=1}^{N(t)}\frac{Q_j}{|r-r_j|} \qquad (3)$$

where $\mathbf{r}_j$ is the center of mass of droplet j, and $\overline{R}(t)$ is the mean radius of the droplets. For a consistent description, $Q_0(t) = \chi(t) - l/\overline{R}(t)$ must be valid at late times.

The growth law of a droplet is obtained by writing a local continuity equation around a volume that encloses only the droplet, $R(dR_i/dt) = Q_i$. The conservation of mass requires

$$\chi(t) + (4\pi/3)\sum_{i=1}^{N(t)} R_i^3 = \phi \qquad (4)$$

where ϕ is the constant volume fraction of the minority phase. The time derivative of this expression is:

$$\frac{\partial\chi(t)}{\partial t} + 4\pi\sum_{i=1}^{N(t)} Q_i + \frac{\partial\chi(t)}{\partial t}\Big|_{nuc} = 0 \qquad (5)$$

The third term is the decrease of $\chi(t)$ due to nucleation of droplets. The second term accounts for the variation of $\chi(t)$ due to growth/dissolution of existing droplets. A mean-field treatment of $\chi(t)$ gives $\Sigma_i Q_i = N\{R(t)\chi(t) - 1\}$ in d = 3, i.e., the background is assumed to be in local equilibrium. Eqs. (3) and (5) represent a set of N + 1 linear coupled equations for the N coefficients Q_i and the coefficient Q_0. The growth equation, the nucleation rate equation, and the conservation law constitute the set of equations used in our simulations. Time evolution starts in an initial supersaturated state, $\chi(t=0) = \phi$. At a given instant t, the nucleation rate, the critical radius, and the growth law, are used to compute the minimum time required to nucleate or eliminate one droplet. This, in turn, determines $\partial\chi/\partial t\,|_{nuc}$. Radii R_i and supersaturation $\chi(t)$ are updated using the resulting minimum dt. This updating of R_i and $\chi(t)$ modifies the minimum dt, which must be computed self-consistently.

Results and Discussion

The time evolution is determined by three parameters: the width dR_c of the nucleation rate distribution function, the nucleation parameter χ_0, and the total volume fraction ϕ. The first two determine the initial radius distribution function and the subsequent cross-over behaviour, while the effects of ϕ persist to late times. The time evolution is divided into three stages: a nucleation, a diffusive growth, and a coarsening stage. Nucleation of droplets produce the initial depletion of the supersaturation. While nucleation is proceeding, the first nuclei start to grow, seizing material from the supersaturation $\chi(t)$. This diffusive growth stage is marked by the high increase in the in slope of $\overline{R}$ (t) and decrease in that of $\chi(t)$, and by a nearly constant droplet density n(t). Finally, when the supersaturation is sufficiently reduced, its role is confined to mediating the exchange of material among the droplets. The critical radius for nucleation becomes slaved to the mean radius of droplets, i.e., $R_c = 1/\chi = \overline{R}$ (t). Growth is a global, interactive phenomenon, and time evolution proceeds through Ostwald ripening [11]: material diffuses away from the smaller, large-curvature droplets (which dissolve), to the larger, low-curvature droplets (which grow). Coarsening is characterized by universal, ϕ-dependent scaling form of the droplet distribution function and by power-law behaviour [1, 12, 13, 16, 18, 20]: $\overline{R}$ (t) = $\{\overline{R}^3(0) + K(\phi)t\}^{1/3}$ and $N(t) = N(0)\overline{R}^3(0)/\{\overline{R}^3(0) + K(\phi)t\}^{-1}$, where the coarsening rate $K(\phi)$ is a monotonically increasing function of ϕ. Figure 1 shows the time evolution for a d = 2 system with volume fraction $\phi = 0.10$.

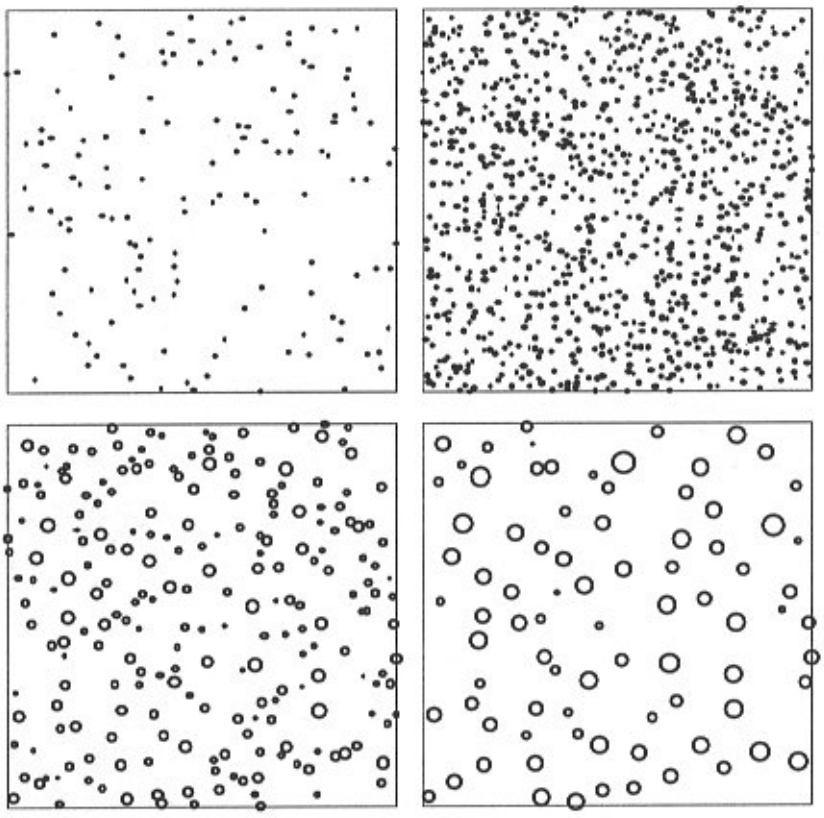

Figure 1. Droplet morphology for a sample d = 2 system, with volume fraction $\phi = 0.05$ and $\chi_0 = 1/3$. **From left to right and top to bottom**, times shown are: t = 40 (nucleation regime), 2,830 (time corresponding to the maximum number of droplets), 63,000 (diffusive regime), and 214,000 (coarsening regime).

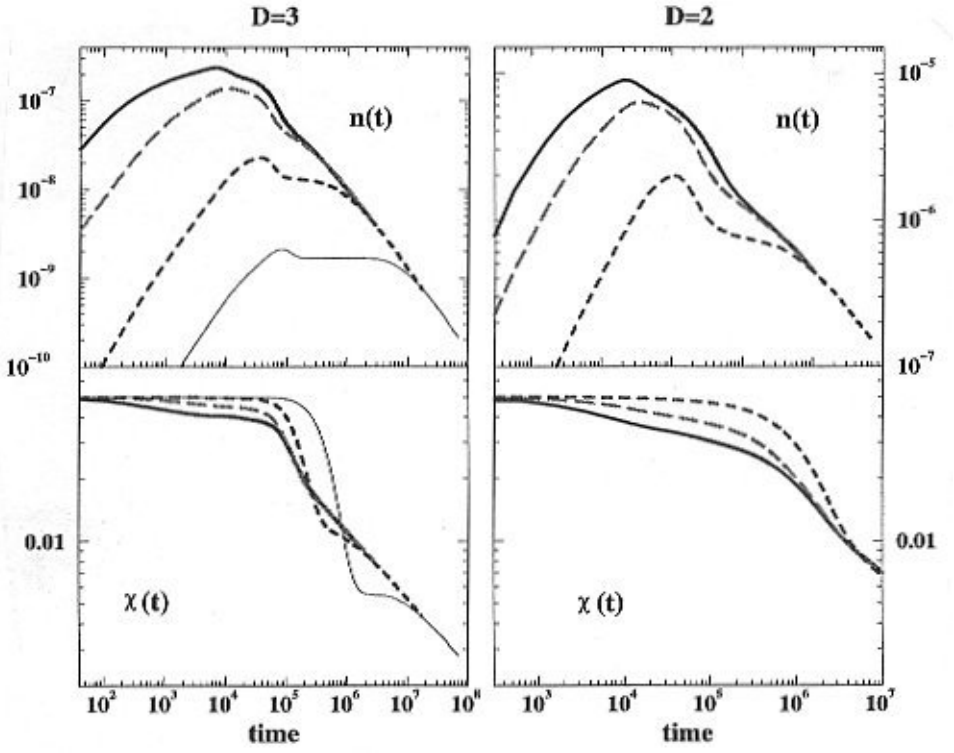

Figure 2. **Top and bottom panels** show the dependence of the droplet density n(t) and the supersaturation $\chi(t)$ on χ_0 for $\phi = 0.05$. **Left column**: d = 3 system with $\chi_0 = 1/7$ (thick solid line), 1/6 (long-dash line), 1/5 (short-dash line), and 1/4.5 (thin solid line). **Right column**: d = 2 system with $\chi_0 = 1/4$ (thick solid line), 1/3 (long-dash line), and 1/2 (short-dash line). Time is measured in units of the

Figure 2 shows the dependence of the droplet density n(t) and the supersaturation $\chi(t)$ on χ_0 for d = 3 and d = 2, and a volume fraction $\phi = 0.05$. As Figure 2 shows, the cross-over to the scaling regime can take several decades in time. The activation energy is given by $E_c/(kT) = \{\chi_0/\chi(t)\}^{(d-1)}$. Thus, the nucleation rate increases and the maximum of n(t) is higher

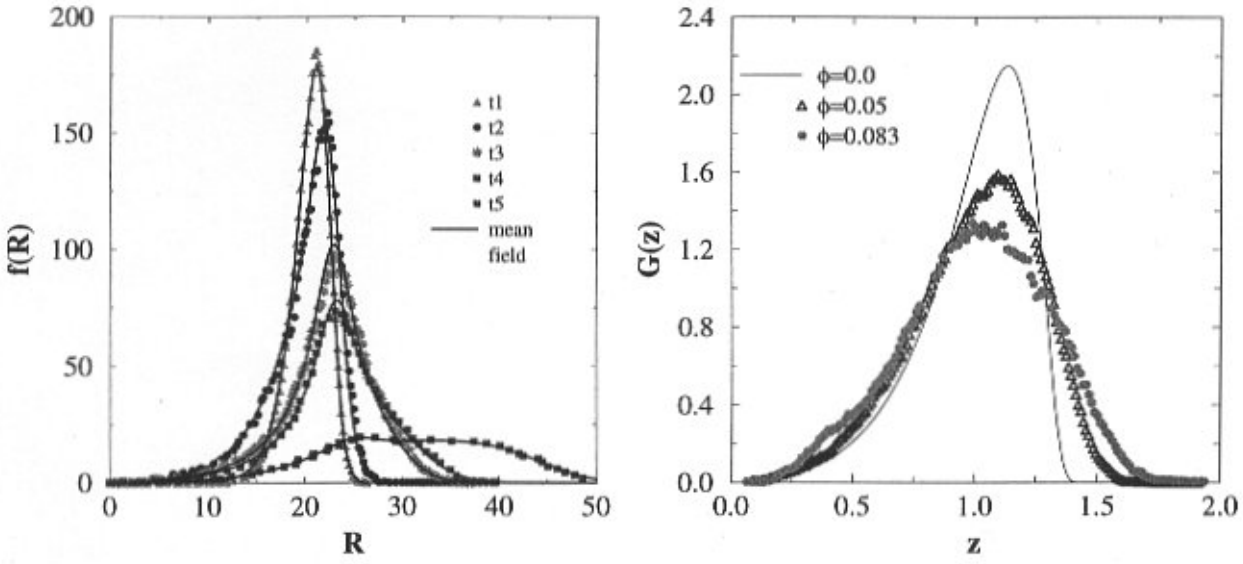

Figure 3. **Left panel**: Early stages for the droplet distribution function for a d = 3 system with $\phi = 0.05$ and $\chi_0 = 1/6$. Times shown are: t1 = 4,785, t2 = 10,675, t3 = 26,582, t4 = 30,648 and t5 = 53,960. On the left-hand-side, note that the distribution function becomes broader with increasing time. The solid line represents the results of our unpublished mean-field theory based on a Thomas-Fermi approximation [20]. **Right panel**: Ripening stage for the previous droplet distribution function (triangles) at $t = 3 \times 10^6$, and for a system with $\phi = 0.083$. The thin solid line corresponds to the Lifshitz-Slyozov result [10]. Time is measured in units of the characteristic diffusion time defined in the text.

---

and occurs sooner with decreasing χ_0 and increasing ϕ. For small ϕ and small χ_0, $\chi(t)$ depletes rapidly initially and diffusive growth is minor, favoring a relative early onset of Ostwald ripening [11] with its characteristic power-law behaviour. However, for larger χ_0, very few droplets with nearly equal radii are nucleated, and the excess of supersaturation is eliminated by the positive growth of all droplets, which hardly interact. Thus, their number stays constant and the droplet distribution function is quite narrow during this stage. After $\chi(t)$ has dropped to very low values, large droplets start growing at the expense of small ones. However, since the droplet distribution function is narrow, it takes some time to introduce a dispersion of radii large enough for n(t) to start to decrease again.

Some early times for the radius distribution functions $f(R,t)$ for d = 3, $\phi = 0.05$ and $\chi_0 = 1/6$ are shown in Figure 3, left panel. With the nucleation of critical droplets, $f(R,t)$ develops a high peak centered at R_c. As supersaturation diminishes, R_c increases and the newly nucleated droplets have larger radii than the older ones, making $f(R,t)$ asymmetric. Before the droplet density n(t) reaches its maximum at t = t2, nucleation is the only mechanism to eliminate the excess of supersaturation. At t2, the size of the initial droplets has fallen well behind the critical size, and their presence produces a long tail for $R < \overline{R}$ (t). These subcritical droplets cost too much surface energy and their dissolution causes the decay of n(t) immediately after t2. However, the system still has quite an excess of supersaturation and nucleation is still an inexpensive way of eliminating it. Between t2 and t4, there is intensive dissolution and creation of droplets. The growth of droplets from the background produces a bump in $f(R,t = t4)$ for large R's, which becomes a second peak between t4 and t5, creating a bimodal distribution $f(R,t)$. This marks the cross-over between the nucleation and the diffusive regimes. After t5, the peak for $R < \overline{R}$ (t) rapidly decreases in height, while the growth peak increases and moves towards larger R's. Finally, the right panel in Figure 3 shows the distribution function for the ripening regime. Also shown in this figure are the Lifshitz-Slyozov [11] results, which corresponds to the limits $\phi = 0$ (this is the ripening stage for the Langer and Schwartz model [10]), and the results of a simulation for $\phi = 0.083$.

Summary

We have introduced a new formalism for nucleation and growth that combines steady-state homogeneous nucleation theory with Ostwald ripening theory [11] and includes the correlations among droplets. The set of self-consistent equations naturally incorporates the cross-over from the early-stage nucleation to the late-stage scaling regime without *ad hoc* assumptions. At present, we are generalizing this formalism for the time evolution of three-dimensional

clusters on d = 2 surfaces, which is especially important for thin film systems [21].

References

[1] Ardell AJ (1990) Late-stage two-dimensional coarsening of circular clusters. Phys. Rev. **B41**, 2554-2556.

[2] Becker R, Döring W (1935) Kinetische Behandlung der Keimbildung in übersättigten Gebilden (Kinetic theory for nucleation of supersaturated structures). Ann. Phys. **24**, 719-752.

[3] Coleman S (1977) Fate of the false vacuum: Semiclassical theory. Phys. Rev. **D15**, 2929-2936.

[4] Farkas L (1927) Keimbildungsgeschwindigkeit in übersättigten Dämpfen (Velocity of nucleation in supersaturated vapors). Z. Physik. Chem. **125**, 236-242.

[5] Gunther NJ, Nicole DA, Wallace DJ (1980) Goldstone modes in vacuum decay and first-order phase transitions. J. Phys. **A13**, 1755-1767.

[6] Gunton JD, Droz M (1983) Introduction to the Theory of Metastable and Unstable States. Lecture Notes in Physics, vol. **183**. Springer-Verlag, Heidelberg, Germany. pp. 49-58.

[7] Kaischew R, Stranski IN (1935) Über den Mechanismus des Gleichgewichts kleiner Kriställchen. II (On the mechanism of the equilibrium of small crystals. II). Z. Physik. Chem. **26**, 114-116.

[8] Langer JS (1967) Theory of the condensation point. Ann. Phys. (NY) **41**, 108-157.

[9] Langer JS (1969) Statistical theory of the decay of metastable states. Ann. Phys. (NY) **54**, 258-275.

[10] Langer JS, Schwartz AJ (1980) Kinetics of nucleation in near-critical fields. Phys. Rev. **A21**, 948-958.

[11] Lifshitz IM, Slyozov VV (1961) The kinetics of precipitation from supersaturated solid solutions. J. Phys. Chem. Solids **19**, 35-50.

[12] Marder M (1987) Correlations and Ostwald ripening. Phys. Rev. **A36**, 858-874.

[13] Marqusee JA, Ross J (1984) Theory of Ostwald ripening: Competitive growth and its dependence on volume fraction. J. Chem. Phys. **80**, 536-543.

[14] Siebert ED, Knobler CM (1984) Measurements of homogeneous nucleation near a critical solution temperature. Phys. Rev. Lett. **52**, 1133-1136.

[15] Siebert ED, Knobler CM (1985) Analysis of light-scattering measurements near a cloud point. Phys. Rev. Lett. **54**, 819-822.

[16] Tokuyama M, Enomoto Y (1992) Dynamics of crossover phenomenon in phase-separating systems. Phys. Rev. Lett. **69**, 312-315.

[17] Volmer M, Weber A (1926) Keimbildung in übersättigten Gebilden (Nucleation of supersaturated structures). Z. Physik. Chem. **119**, 277-301.

[18] Voorhees PW (1985) The theory of Ostwald ripening. J. Stat. Phys. **38**, 231-252.

[19] Wong NC, Knobler CM (1978) Light scattering studies of phase separation in isobutyric acid + water mixtures. J. Chem. Phys. **69**, 725-735.

[20] Yao JH, Elder KR, Guo H, Grant M (1992) Ostwald ripening in two and three dimensions. Phys. Rev. **B45**, 8173-8176.

[21] Zinke-Allmang M, Feldman LC, Grabow MH (1992) Clustering on surfaces. Surf. Sci. Rep. **16**, 377-458.

Discussion with Reviewers

T. Lookman: How good is the approximation when the results are compared to experimental observations?
Authors: We hope that our paper will motivate careful experiments on the issue.

Reviewer II: In relation to correlations effects: the authors state several times in the paper that they include the effects of the correlation of droplets; can correlation effects be presented.
Authors: All our figures include those correlation effects and are different from those that would be obtained in absence of such correlations. The right panel to Figure 3 shows one possible comparison.

Reviewer II: These simulations represent the cross-over regime between early stage nucleation and late stage ripening. As support for the correct form of such a cross-over, do the authors find that the details of late stage ripening in their model (i.e., the droplet size distribution), approach ripening predictions at late times?
Authors: In fact, the details of the late stage ripening in our model closely approach the ripening predictions at late times. Comparisons will be presented elsewhere.

Reviewer II: The solid lines in Figure 3 are the results of a mean field theory that includes droplet correlation effects. Can you comment further on the terminology used? Does a mean field theory not ignore correlations?
Authors: The mean-field theory used by, say, Lifshitz-Slyozov theory [11] or Langer-Schwartz theory [10], considers a single droplet and the effect of all other droplets only appear through the droplet distribution function. As a consequence, some of the predictions, such as, the shape of the distribution function or the slope of the mean radius, are only valid when the volume fraction $\phi \to 0$. For non-zero ϕ, the steady state problem for ripening resembles a homogeneous electron gas, since droplets interact via the Laplace equation in the steady-state limit and charge neutrality is invoked. Yao *et al.* [20] introduced screening effects among the droplets and approximated the many-droplet correlation effects in the same manner as the Thomas-Fermi mechanism for Coulomb systems. Our

approach is an extension of that work [20].

Reviewer II: I am rather surprised that the mean field predictions plotted in Figure 3 agree so well with simulations that have droplet interactions. I would have thought that the inclusions of the interactions would alter the results. In fact, the agreement appears so good that I do not see why the simulations are even required!

Authors: How the mean field predictions compare with simulations depends on the parameter and time regimes. For instance, for the case shown with volume fraction $\phi = 0.05$, the comparison is good for values of the nucleation parameter $\chi_0 \leq 1/6$ and becomes poor for larger values of χ_0. Also, the comparison is poorer with volume fractions $\phi > 0.05$. The simulations within the limits of the model always give the exact results. The Thomas-Fermi approach give approximate results, quite good for certain parameters regimes, and thus, provide an inexpensive way of obtaining rough estimates. Further discussions of the mean field approach and its limitations are scheduled for another publication.

Reviewer II: The following points are concerned with how the authors have dealt with small cluster sizes in their simulations. (**a**). What is the smallest droplet size allowed in the simulations? Since the nucleation stage includes a Gaussian distribution of droplet sizes, it appears that sizes arbitrarily close to zero are permitted. The droplet size distributions in Figure 3 also indicate this since they appear to fall gradually to zero as the droplet size decreases. (**b**). Why is a Gaussian distribution of droplet sizes chosen for the nucleation stage? This allows for droplets which are less than the critical size which are unstable and should not nucleate at all! What happens to these unstable droplets and why are they introduced in the first place? (**c**). The Gibbs-Thomson boundary condition is valid only for "large" droplets since the supersaturation diverges as the particle size approaches zero. During the nucleation stage and during ripening stages of growth (where droplet dissolution occurs) some very small drop-lets seem present. When does the divergence in the su-persaturation caused by the boundary condition become unphysical? Do the authors take this into account? (**d**). I find it very curious that during the ripening stages of the simulations, the particle dissolution results in a locally high enough supersaturation to create a "second nucleation stage". It seems that if ripening processes result in particle dissolution, then why would a new droplet nucleate? Would the large droplet nearby (which is causing the dissolution of the small droplet) not prevent re-nucleation?

Authors: (**a**). The droplet size in the simulation is picked from a quite narrow Gaussian random number distribution, of width dR_c. Sizes arbitrarily close to zero have a small chance of occurring. The droplets distribution functions in the second panel of Figure 3 are obtained as an average over 30 runs. The resulting distribution function is further smoothed using standard filtering techniques. This extrapolates the droplet distribution function smoothly to zero. In the scale shown in Figure 3, the error bars are of order of 4 units. (**b**). The model can flexibly admit any choice of distribution function for the nucleation rate; a Gaussian distribution is customarily assumed in the standard literature. Subcritical droplets can be nucleated (they eventually dissolve) and they provide an important source of fluctuations. A distribution function that allows subcritical droplets is also consistent with the late-stage distribution function, where the critical radius becomes the mean radius. Langer and Schwartz [10] also discuss this point. (**c**). No divergence of the supersaturation at the droplet interface is ever observed for the simple reason that long before that stage the droplet is energetically not favored and dissolves. This is taken into account by considering the growth law of each individual droplet: $R(t + dt) = R(t) + d \cdot dtQ_i(t)$. For very small droplets, $Q_i(t)$ is a very large negative number. Thus, we can compute a minimum time dt_{min} for the disappearance of a droplet: $dt_{min} = -R_{in}(t)/\{d\, Q_{min}(t)\}$. Integration of the equations is performed in very small, variable time steps dt. When $dt = dt_{min}$, all those droplets, whose radius would be zero after the time integration, are eliminated from the system. (**d**). This is a misinterpretation. There is no second nucleation stage during the ripening stages. The bimodal distribution shown in Figure 3 signals the cross-over from the nucleation-dominated regime to the diffusion-dominated regime. The ripening regime for this system is shown in right panel of Figure 3 to further illustrate this point.